Journal of Nano- and Electronic Physics
Vol. **14** No 2, 02013(6pp) (2022)

Журнал нано- та електронної фізики
Том **14** № 2, 02013(6cc) (2022)

Optical Conductivity of Spherical Metal Nanoparticles Taking into Account the Size Dependence of the Fermi Energy

A.O. Koval[1,2,*]

[1] *Zaporizhzhia Polytechnic National University, 64, Zhukovskogo St., 60063 Zaporizhzhia, Ukraine*
[2] *Scientific and Production Complex "Iskra", 84, Mahistralna St., 69071 Zaporizhzhia, Ukraine*

(Received 21 December 2021; revised manuscript received 17 April 2022; published online 29 April 2022)

The interaction of electromagnetic waves with a spherical metal nanoparticle is studied in this work. Within the model of a finite spherically symmetric potential well, the dimensional dependence of the Fermi energy of conduction electrons is calculated. It has been shown that taking into account the model of a finite spherical potential well leads to a decrease in the value of the Fermi energy, while the general character of the size dependences is preserved. In the diagonal response approximation, the expressions are obtained and the diagonal components of the optical conductivity tensor of a spherical metal nanoparticle with radius r_0 are calculated. The influence of the variation of the effective radius and the material of a spherical nanoparticle on the frequency dependences of the real and imaginary parts of the optical conductivity has been investigated. By comparing the results of calculations of the diagonal component of the optical conductivity tensor of a spherical nanoparticle and a cylindrical nanowire for Cu, the influence of the dimensionality of the systems is established. The results of the calculations show a strong dimensional and frequency dependence of the real and imaginary parts of the optical conductivity. The calculations are performed for Ag, Cu and Al spherical nanoparticles. The differences in the results for Ag, Cu and Al spherical nanoparticles are explained by different values of the relaxation time of conduction electrons.

Keywords: Fermi energy, Metallic nanoparticle, Optical conductivity, Size quantization.

DOI: 10.21272/jnep.14(2).02013 PACS numbers: 61.46.Bc, 73.22. – f

1. INTRODUCTION

Studies of the optical properties of small metal particles are traditionally considered relevant [1-3]. First of all, this is due to their use in optical and electronic devices of new generation, in particular, in the creation of metamaterials [4], in sensor technology [5], memory cells [6], high-speed optoelectronics [7] and superlenses [8]. In addition, metal nanoparticles are directly used in medical diagnostics [9].

Nowadays, experimental methods have been developed to study the optical-spectral characteristics of individual metal nanoparticles [10, 11]. Studies of the optical properties of metal nanoparticles and their ensembles provide important information on the structure of the electronic levels of the energy spectrum and the position of the Fermi level in such nanostructures. New technologies make it possible to obtain ensembles of nanoparticles with a radius of several tens to hundreds of nanometers in the form of flattened or elongated ellipsoids of rotation, disc-shaped forms, etc. [12, 13]. The simplest case in the study are spherical nanoparticles. However, obtaining particles identical in their parameters still remains an unsolved problem.

Metal nanoparticles have unique optical and spectral properties. Varying the shape and size of small particles can significantly enhance the optical response of low-dimensional systems [14-17]. The spectroscopic properties directly depend on the environment in which the nanoparticles are located [18]. Due to the application of metal or semiconductor shells to the dielectric core, it is possible to regulate the position and peak of resonant absorption in such structures.

The basic parameters for calculating the spectra of metal nanoparticles are the real and imaginary parts of the optical conductivity. Theoretical works devoted to the study of the optical properties of metal nanoparticles are based on the analysis of both classical [19] and quantum-dimensional effects [20, 21]. A comparison of different quantum-mechanical approaches which allow to study the optical response of nanoobjects is given in [22]. One of the theories that considers the reaction of nanoparticles in the form of parallelepipeds to an external electromagnetic field is the Wood-Ashcroft theory [23].

In this work, in the framework of the diagonal response to an electromagnetic wave, the diagonal components of the optical conductivity of a spherical metal nanoparticle are calculated taking into account the dimensional dependence of the position of the Fermi level in the metal. For this reason, the approach [23] is used, which is adapted for ultra-thin films and wires in [24]. This model can be used to study a dielectric particle covered with a thin layer of metal or semiconductor shell.

2. BASIC RELATIONS

The current induced by an electromagnetic wave with a frequency ω and a wave vector $\mathbf{q}$ is defined by the formula:

$$j_{\mu\nu} = \sum_{\nu} \sigma_{\mu\nu}(\mathbf{q},\omega) E_{\nu}, \qquad (1)$$

where $\sigma_{\mu\nu}$ is the conductivity tensor, and E_{ν} are the electric field components.

Using the results of [24], the diagonal components of the conductivity tensor can be represented as

$$\sigma_{\mu\mu} = \frac{\mathrm{i}e^2\bar{n}}{m_e\omega} + \frac{2\mathrm{i}e^2}{m_e^2\omega\Omega}\sum_{i,j}\frac{f_i\varepsilon_{ij}}{\varepsilon_{ij}^2-\hbar^2\omega^2}\left\langle j\left|\hat{p}_{\mu}\right|i\right\rangle^2, \qquad (2)$$

* andrej.koval@ukr.net

where e is the electron charge; $\bar{n}$ is the density of conduction electrons; $\Omega = 4\pi r_0^3/3$ is the volume of the particle; $i = \sqrt{-1}$; $\mu = x, y, z$; m_e is the mass of an electron; $f_i = \left[\exp\left((\varepsilon_i - \varepsilon_\mathrm{F})/k_\mathrm{B}T\right)+1\right]^{-1}$ is the fill factor of the state with an energy ε_i; $|i\rangle \equiv |n,l,m\rangle$ and $\langle j| \equiv \langle n',l',m'|$ are the vectors of the initial and final states; $\varepsilon_{ij} = \varepsilon_i - \varepsilon_j$; $\langle j|\hat{p}_\mu|i\rangle$ is the matrix element of projections of the momentum operator and T is the temperature. Further, we assume that $T = 0$.

It is assumed that the conduction electrons of the nanoparticle are located in a spherically symmetric rectangular well with a depth $U_0 < 0$. In this case, the solution of the Schrödinger equation has the form

$$\psi_{nlm}(r,\theta,\varphi) = R_{nl}(r)Y_{lm}(\theta,\varphi), \tag{3}$$

where the radial dependence of the wave function is

$$R_{nl}(r) = \begin{cases} C_{nl} j_l(k_{nl} r), & r \le r_0; \\ B_{nl} h_l^{(1)}(\mathrm{i}\varkappa_{nl} r), & r > r_0, \end{cases} \tag{4}$$

$k_{nl} = \sqrt{k_0^2 - \varkappa_{nl}^2}$, $\hbar k_0 = \sqrt{2m_e|U_0|}$, j_l is the spherical Bessel function of the l-th order, $h_l^{(1)}$ is the spherical Hankel function of an imaginary argument. The subscript $n = 1,2,\ldots$ enumerates the roots of the characteristic equation for a given l value, which follows from the condition of continuity of the logarithmic derivative of the wave function at the well boundary:

$$k_{nl}\frac{j_l'(k_{nl}r_0)}{j_l(k_{nl}r_0)} = \varkappa_{nl}\frac{h_l'^{(1)}(\mathrm{i}\varkappa_{nl}r_0)}{h_l^{(1)}(\mathrm{i}\varkappa_{nl}r_0)}, \tag{5}$$

where the prime denotes differentiation with respect to the entire argument.

Spherical harmonics are described by the expression

$$Y_{lm}(\theta,\varphi) = \sqrt{\frac{2l+1}{4\pi}\frac{(l-m)!}{(l+m)!}}P_l^m(\cos\theta)\mathrm{e}^{\mathrm{i}m\varphi}, \tag{6}$$

where $m = 0, \pm1, \pm2 \ldots \pm l$, and $P_l^m(\cos\theta)$ is the associated Legendre function.

By using formulas (3)-(6), after rather cumbersome transformations, the matrix elements of different projections of the momentum operator can be expressed in the form:

$$\langle j|\hat{p}_\mu|i\rangle = \begin{cases} -\mathrm{i}\hbar\delta_{mm'}\left\{\mathscr{G}_{(-)}\mathscr{L}_{(1)}\delta_{l-1,l'} - \mathscr{G}_{(+)}\mathscr{L}_{(2)}\delta_{l+1,l'}\right\}, & \mu = z; \\ -\mathrm{i}\dfrac{\hbar}{2}\left\{\mathscr{G}_{(-)}\mathscr{M}_{(-)}\delta_{l-1,l'} + \mathscr{G}_{(+)}\mathscr{N}_{(-)}\delta_{l+1,l'}\right\}, & \mu = x; \\ -\dfrac{\hbar}{2}\left\{\mathscr{G}_{(-)}\mathscr{M}_{(+)}\delta_{l-1,l'} + \mathscr{G}_{(+)}\mathscr{N}_{(+)}\delta_{l+1,l'}\right\}, & \mu = y, \end{cases} \tag{7}$$

where

$$\mathscr{G}_{(\mp)} = k_{nl}C_{nl}C_{n',l\mp1}\int_0^{r_0} j_{l\mp1}(k_{n',l\mp1}r)j_{l\mp1}(k_{nl}r)r^2dr \mp \varkappa_{nl}B_{nl}B_{n',l\mp1}\frac{\pi^2}{4}\int_{r_0}^{\infty} h_{l\mp1}^{(2)}\left(e^{-\mathrm{i}\frac{\pi}{2}}\varkappa_{n',l\mp1}r\right)h_{l\mp1}^{(1)}\left(e^{\mathrm{i}\frac{\pi}{2}}\varkappa_{nl}r\right)r^2dr,$$

$$\mathscr{L}_{(1)} = \sqrt{\frac{(l-m)(l+m)}{(2l-1)(2l+1)}}, \qquad \mathscr{L}_{(2)} = \sqrt{\frac{(l-m+1)(l+m+1)}{(2l+1)(2l+3)}},$$

$$\mathscr{F}_{(\mp)}^{(1)} = \sqrt{\frac{(l\mp m-1)(l\mp m)}{(2l-1)(2l+1)}}, \quad \mathscr{F}_{(\mp)}^{(2)} = \sqrt{\frac{(l\mp m+1)(l\mp m+2)}{(2l+1)(2l+3)}},$$

$\mathscr{M}_{(\mp)} = \mathscr{F}_{(-)}^{(1)}\delta_{m+1,m'} \mp \mathscr{F}_{(+)}^{(1)}\delta_{m-1,m'}$,

$\mathscr{N}_{(\mp)} = \mathscr{F}_{(+)}^{(2)}\delta_{m+1,m'} \mp \mathscr{F}_{(-)}^{(2)}\delta_{m-1,m'}$, and $\delta_{\mu\nu}$ is the Kronecker symbol.

It is easy to see that, for a fixed direction of polarization, the summation in (2) over all m (and m') does not depend on the direction. Therefore,

$$\sum_m \left|z_{nlm}^{n',l-1,m}\right|^2 = \mathscr{G}_{(-)}^2\sum_{m=-l}^{l}\mathscr{L}_{(1)}{}^2 = \frac{l}{3}\mathscr{G}_{(-)}^2;$$

$$\sum_m \left|z_{nlm}^{n',l+1,m}\right|^2 = \mathscr{G}_{(+)}^2\sum_{m=-l}^{l}\mathscr{L}_{(2)}{}^2 = \frac{l+1}{3}\mathscr{G}_{(+)}^2;$$

$$\sum_m \left|x_{nlm}^{n',l-1,m+1}\right|^2 + \left|x_{nlm}^{n',l-1,m-1}\right|^2$$

$$= \mathscr{G}_{(-)}^2\sum_{m=-l}^{l}\frac{1}{2}\left(\left(\mathscr{F}_{(-)}^{(1)}\right)^2 + \left(\mathscr{F}_{(+)}^{(1)}\right)^2\right) = \frac{l}{3}\mathscr{G}_{(-)}^2;$$

$$\sum_m \left|x_{nlm}^{n',l+1,m+1}\right|^2 + \left|x_{nlm}^{n',l+1,m-1}\right|^2$$

$$= \mathscr{G}_{(+)}^2\sum_{m=-l}^{l}\frac{1}{2}\left(\left(\mathscr{F}_{(+)}^{(2)}\right)^2 + \left(\mathscr{F}_{(-)}^{(2)}\right)^2\right) = \frac{l+1}{3}\mathscr{G}_{(+)}^2;$$

Then, the squared matrix element of the projection of the momentum operator (7) is also independent of the direction and has the form:

$$\left|\langle j|\hat{p}_\mu|i\rangle\right|^2 = \frac{\hbar^2}{3}\left\{l\mathscr{G}_{(-)}^2\delta_{l-1,l'} + (l+1)\mathscr{G}_{(+)}^2\delta_{l+1,l'}\right\}. \tag{8}$$

Given the absorption by substitution $\omega \to \omega + \mathrm{i}/\tau$ (τ is the relaxation time) in expression (2), we obtain the formula for the diagonal component of the optical conductivity

$$\sigma_{\mu\mu} = \sigma_{DR}\left\{1 + S(\omega, r_0)\right\}, \tag{9}$$

where

$$S(\omega,r_0) = \frac{2}{Nm_e}\sum_{i,j}\frac{f_i\varepsilon_{ij}\left(\varepsilon_{ij}^2 - \hbar^2\omega^2 + \dfrac{\hbar^2}{\tau^2} + \dfrac{2\mathrm{i}\hbar^2\omega}{\tau}\right)}{\left(\varepsilon_{ij}^2 - \hbar^2\omega^2 + \dfrac{\hbar^2}{\tau^2}\right)^2 + \dfrac{4\hbar^4\omega^2}{\tau^2}}\left|\langle j|\hat{p}_\mu|i\rangle\right|^2,$$

$\sigma_{DR} = \sigma(0)\dfrac{1+\mathrm{i}\omega\tau}{1+\omega^2\tau^2}$ is the Drude formula and $\sigma(0) = e^2\bar{n}\tau/m_e$ is the static conductivity.

The real and imaginary parts of the optical conductivity can be finally written as:

$$\mathrm{Re}\,\sigma_{\mu\mu} = \frac{2e^2\overline{n}}{\hbar}\frac{k_\tau^2}{k_\omega^4+k_\tau^4}\left(1+\frac{4}{\hbar^2 N}\sum_{i,j}f_i\frac{\left(k_{nl}^2-k_{n'l'}^2\right)\left(\left(k_{nl}^2-k_{n'l'}^2\right)^2-3k_\omega^4+k_\tau^4\right)}{\left(\left(k_{nl}^2-k_{n'l'}^2\right)^2-k_\omega^4+k_\tau^4\right)^2+4k_\omega^4k_\tau^4}\left|\langle j|\hat{p}_\mu|i\rangle\right|^2\right), \tag{10}$$

$$\mathrm{Im}\,\sigma_{\mu\mu} = \frac{2e^2\overline{n}}{\hbar}\frac{k_\omega^2}{k_\omega^4+k_\tau^4}\left(1+\frac{4}{\hbar^2 N}\sum_{i,j}f_i\frac{\left(k_{nl}^2-k_{n'l'}^2\right)\left(\left(k_{nl}^2-k_{n'l'}^2\right)^2-k_\omega^4+3k_\tau^4\right)}{\left(\left(k_{nl}^2-k_{n'l'}^2\right)^2-k_\omega^4+k_\tau^4\right)^2+4k_\omega^4k_\tau^4}\left|\langle j|\hat{p}_\mu|i\rangle\right|^2\right). \tag{11}$$

where $k_\omega^2 = 2m_e\omega/\hbar$, $k_\tau^2 = 2m_e/\hbar\tau$, and the fill factor is approximated by the step function $f_{nlm} = \Theta\left(\varepsilon_\mathrm{F}-\varepsilon_{nlm}\right)$.

The diagonal component of the conductivity tensor is calculated by formulas (10) and (11) using expression (8) for the squared matrix element of the projection of the momentum operator.

We obtain the transcendental equation for determining the Fermi energy ε_F [25]:

$$\overline{n}\Omega = \sum_{\kappa=1}^{\infty}\frac{4}{\pi\kappa}\left(1-\cos\pi\kappa\right)\sum_{n,l}\sin\frac{\pi\kappa\varepsilon_{nl}}{\varepsilon_\mathrm{F}}. \tag{12}$$

It is assumed that the density of conduction electrons in a nanoparticle is the same as in an infinite metal. Summation is performed over all n and l for which

$$\varepsilon_{nl} = \frac{\hbar^2}{2m_e r_0^2}\chi_{nl}^2 \le \varepsilon_\mathrm{F}. \tag{14}$$

3. RESULTS OF THE CALCULATIONS AND DISCUSSION

The calculations were performed for electron concentrations $\overline{n} = \left(4\pi r_s^3/3\right)^{-1}$, where $r_s = 3{,}02a_0$; $2{,}67a_0$ and $2{,}07a_0$ (a_0 is the Bohr radius) for the Ag, Cu and Al metals, respectively.

Fig. 1 shows the size dependences of the Fermi energy of Ag and Al nanoparticles. These dependences exhibit an "oscillatory" behavior. Taking into account the model of the finite potential well leads to a decrease in the value of the Fermi energy level. Increasing the radius of the particle leads to a decrease in the period and amplitude of oscillations, the values of which approach the value of the Fermi energy in a 3D metal $\left(\varepsilon_{\mathrm{F}_0} = \hbar^2k_{\mathrm{F}_0}^2/2m_e\right)$.

The specific features of the size dependences of the Fermi energy for Ag and Al nanoparticles are determined only by different values of electron concentration $\overline{n}$ of these metals. Compared to the Ag particle, the scale of the oscillation period for the Al particle is smaller, because the root distribution density k_{nl} is higher.

Fig. 2 shows the frequency dependences of Ag nanoparticles with a radius $r_0 = 1$ and 2 nm (curves 1, 2 and 3, 4, respectively). At such radii, the peaks correspond to transitions between the size quantization levels. Taking into account the model of the finite potential well (dashed curves in Fig. 2), all peaks are shifted to lower frequencies. The reason is the decrease in energy levels, as a result of which the distance between them decreases and the optical transitions begin at lower frequencies.

Increasing the radius also shifts to lower frequencies, and the frequency range occupied by the peaks decreases. The peaks begin to merge with each other, and their number decreases. The position of the peaks is predictable, even though the spectrum of k_{nl} is rather complex.

For example, we determine for Ag nanoparticle the position of the peak with the highest height in the dependence of the quantity $\mathrm{Re}\,\sigma_{\mu\mu}$.

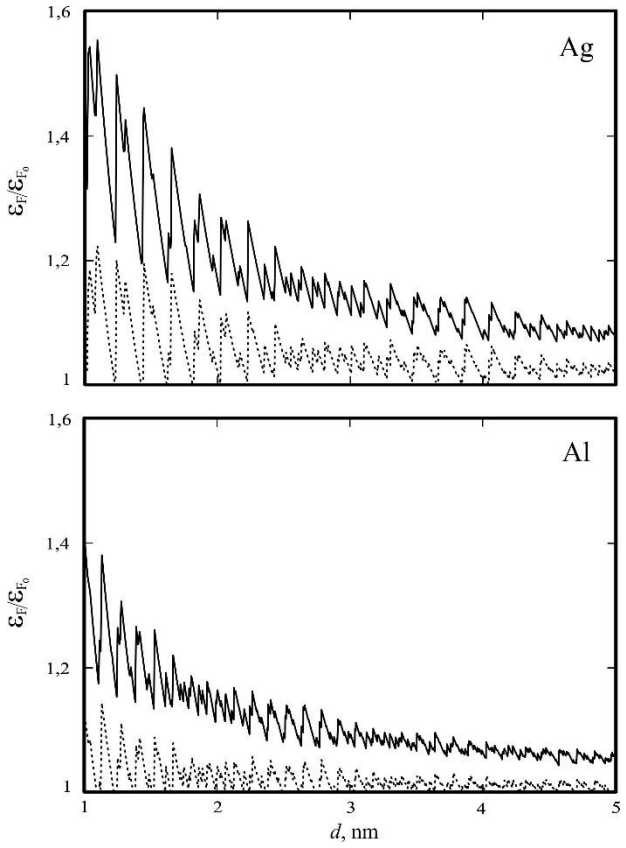

Fig. 1 – Size dependences of the Fermi energy for Ag and Al nanoparticles (solid lines are the model of the infinite potential well; dashed lines are the model of the finite potential well)

The height of the peaks is proportional to the square of the matrix element of the operator $\hat{p}_\mu$, and the matrix element has a maximum value at $n' = n$ since the corresponding integral in (8) under this condition is

maximum. Thus, the maximum value of $\mathrm{Re}\,\sigma_{\mu\mu}$ is attained at $l=0$ and $n'=n=n_{\mathrm{F}}$. Assuming that $k_{\mathrm{F}}\approx k_{\mathrm{F}_0}=\left(3\pi^2\bar{n}\right)^{1/3}$, we find that $n_{\mathrm{F}}\approx k_{\mathrm{F}_0}r_0/\pi=3$ for $r_0=1$ nm. As a result,

$$\hbar\omega_{\max}=\frac{\hbar^2\left(k_{3,1}^2-k_{3,0}^2\right)}{2m_e}=\frac{\hbar^2\left(\chi_{3,1}^2-\chi_{3,0}^2\right)}{2m_e r_0^2}=1{,}14\ \text{eV}.$$

An error of about 10 % is due to the assumption of a uniform distribution of levels.

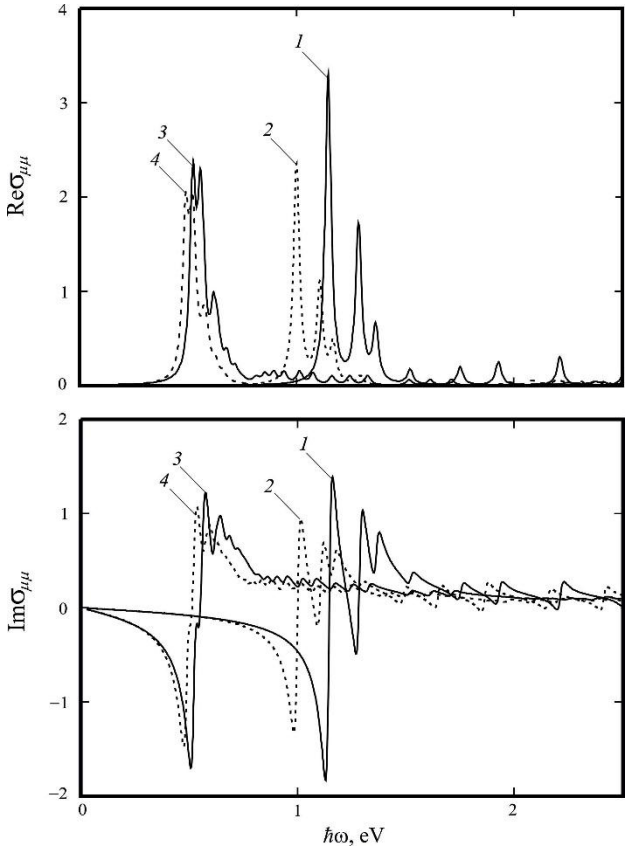

Fig. 2 – Frequency dependences of the real and imaginary parts of the optical conductivity of the Ag nanoparticle: solid lines are the model of the infinite potential well; dashed lines are the model of the finite potential well. The radii of nanoparticles are (1, 2) r_0 = 1 nm and (3, 4) r_0 = 2 nm

Let us compare the conductivity tensor components in order of magnitude for the Ag nanoparticle. We take into account that $\varepsilon_{ij}=\hbar\omega$, $\hbar^2\omega^2<<\hbar^2/\tau^2$ and that the following relationships from (9) are valid:

$$\mathrm{Re}\,\sigma_{\mu\mu}=\sigma_{DR}\,\mathrm{Im}\,S\left(\omega,r_0\right), \tag{14}$$

where $\mathrm{Im}\,S\left(\omega,r_0\right)\approx\dfrac{\tau}{\hbar N m_e}\sum\limits_{i,j}f_i\left|\left\langle j\right|\hat{p}_\mu\left|i\right\rangle\right|^2$.

Then, with the use of the expression $\left|\left\langle j\right|\hat{p}_\mu\left|i\right\rangle\right|^2\cong\dfrac{\hbar^2k_{\mathrm{F}_0}^2}{3}\left(2l+1\right)$, we obtain

$$\mathrm{Im}\,S\left(\omega,r_0\right)\approx\frac{\tau\hbar k_{\mathrm{F}_0}^2}{4\pi r_0^3\bar{n}m_e}\sum_l(2l+1). \tag{15}$$

At $\hbar\omega=1{,}14$ eV and the frequency of absorption $\hbar/\tau=0{,}016$ eV we obtain that the static conductivity $\sigma(0)=5{,}91\cdot10^{17}\mathrm{s}^{-1}$ and $\sigma_{DR}\cong\sigma(0)/\omega\tau\cong0{,}85\cdot10^{16}\mathrm{s}^{-1}$. Hereinafter $e^2/2a_0\hbar=2{,}1\cdot10^{16}\mathrm{s}^{-1}$ will be used as a conductivity unit. Then, we have $\sigma_{DR}\cong0{,}41$.

Substituting $\tau=4\cdot10^{-14}$s (for the Ag nanoparticle) and $r_0=1$ nm into (15), we obtain $\mathrm{Im}\,S\left(\omega,r_0\right)\cong8{,}1$ and $\mathrm{Re}\,\sigma_{\mu\mu}\cong3{,}2$. This value is in good agreement with the calculated data presented in Fig. 2 (the first maximum in curve 1). In the macroscopic limit $r_0=\infty$ we have $\mathrm{Re}\,\sigma_{\mu\mu}=0$, $\mathrm{Im}\,\sigma_{\mu\mu}=\mathrm{Im}\,\sigma_{DR}$.

Fig. 2 demonstrates the important fact that $\mathrm{Re}\,\sigma_{\mu\mu}$ is nonnegative in the entire investigated frequency range, while $\mathrm{Im}\,\sigma_{\mu\mu}$ is an alternating function of frequency.

Fig. 3 shows the results of $\mathrm{Re}\,\sigma_{\mu\mu}$ for metal nanoparticles with similar results for a thin metal wire [24]. For a wire of radius ρ_0, for $\alpha=x,y$, the squared matrix element of the projection of the momentum operator has the form

$$\left|\left\langle j\right|\hat{p}_\alpha\left|i\right\rangle\right|^2=\frac{\hbar^2}{4}\delta_{pp'}\left\{\mathscr{F}_{(-)}^{-2}\delta_{m-1,m'}+\mathscr{F}_{(+)}^{-2}\delta_{m+1,m'}\right\},$$

$$\mathscr{F}_{(\mp)}=k_{mn}C_{mn}C_{m\mp1,n'}\int_0^{\rho_0}I_{m\mp1}\left(k_{m\mp1,n'}\rho\right)I_{m\mp1}\left(k_{mn}\rho\right)\rho d\rho$$

$$\mp\varkappa_{mn}B_{mn}B_{m\mp1}\int_{\rho_0}^{\infty}K_{m\mp1}\left(\varkappa_{m\mp1,n'}\rho\right)K_{m\mp1}\left(\varkappa_{mn}\rho\right)\rho d\rho,$$

where $k_{mn}=\sqrt{k_0^2-\varkappa_{mn}^2}$, I_m is the Bessel function and K_m is the Macdonald function. The number $n=1,2\ldots$ enumerates the roots of the characteristic equation for a given m value:

$$k_{mn}\frac{I_m'\left(k_{mn}\rho_0\right)}{I_m\left(k_{mn}\rho_0\right)}=\varkappa_{mn}\frac{K_m'\left(\varkappa_{mn}\rho_0\right)}{K_m\left(\varkappa_{mn}\rho_0\right)}.$$

The differences in the position and size of the peaks are explained by the different energy spectra of the 0D and 1D systems. After the recalculation in the 0D system, there remains the summation over the quantum numbers n and l, and, in the case of the 1D system, n and m.

Assuming that $\left|\left\langle m'n'\right|\hat{p}_\alpha\left|mn\right\rangle\right|^2\cong\hbar^2k_{\mathrm{F}_0}^2/4$ and $\sum\limits_p1\cong2Lk_{\mathrm{F}_0}/\pi$, we obtain

$$\frac{\mathrm{Re}\,\sigma_{\mu\mu}^{\mathrm{sphere}}}{\mathrm{Re}\,\sigma_{\alpha\alpha}^{\mathrm{wire}}}\cong\frac{\Omega_{0\mathrm{D}}^{-1}\sum_{i,j}\left|\left\langle n'l'\right|\hat{p}_\mu\left|nl\right\rangle\right|^2}{\Omega_{1\mathrm{D}}^{-1}\sum_{i,j}\left|\left\langle m'n'\right|\hat{p}_\alpha\left|mn\right\rangle\right|^2\sum_p1}=\frac{k_{\mathrm{F}_0}^2\sum_l(2l+1)}{6\pi r_0\bar{n}}.$$

For Cu at $r_0 = \rho_0 = 1$ nm and $k_{F_0} \cong 1{,}36 \cdot 10^{10}$ m^{-1} ($n_F = 4$; $l = 0 \ldots n_F - 1$) we have

$$\mathrm{Re}\,\sigma_{\mu\mu}^{\mathrm{sphere}} \Big/ \mathrm{Re}\,\sigma_{\alpha\alpha}^{\mathrm{wire}} \cong 1{,}9.$$

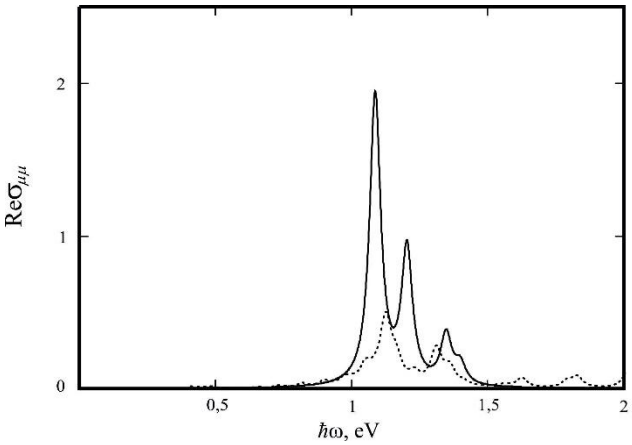

Fig. 3 – Frequency dependences of the optical conductivity real part of the Cu nanoparticle (solid line) and the Cu nanowire (dashed line) with radii $r_0 = \rho_0 = 1$ nm

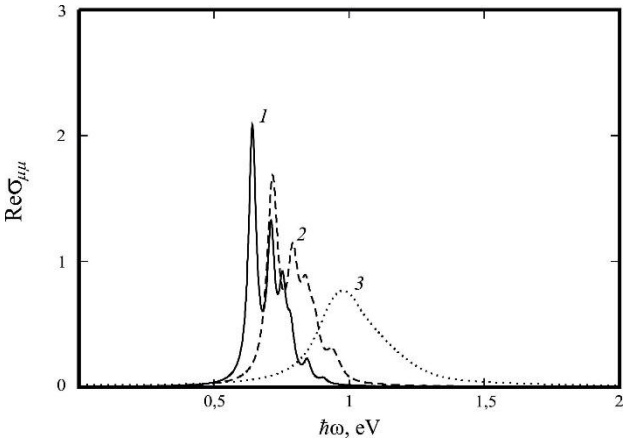

Fig. 4 – Frequency dependence of the optical conductivity real part for nanoparticles of various metals: 1 – Ag, 2 – Cu,3 – Al

The frequency dependences of the real part of the optical conductivity for different metals at a fixed particle radius (r_0 = 1,5 nm) are shown in Fig. 4. The results obtained are qualitatively and quantitatively different for Ag, Cu, and Al particles. In particular, in the case of Ag and Cu nanoparticles, in contrast to Al ones, there are strong oscillations in almost the entire frequency range under consideration. This is explained by the short relaxation time of electrons $\tau = 2{,}07 \cdot 10^{-14}$s in Al, so that the width of the peaks is $\hbar/\tau = 0{,}082$ eV. In this regard, Ag $(\hbar/\tau = 0{,}016\ \mathrm{eV})$ has the least value. In calculations, we used the electron relaxation times τ taken from [26] for 3D metals.

Despite the absence of peaks in the frequency dependence of the conductivity for the Al nanoparticle, the maximum of this dependence can be determined taking into account that $n_F = 8$. Then, for $r_0 = 1{,}5$ nm, we have

$$\hbar\omega_{\max} = \frac{\hbar^2\left(\chi_{8,1}^2 - \chi_{8,0}^2\right)}{2m_e r_0^2} = 1{,}3\ \mathrm{eV}.$$

The obtained result agrees well with the calculation results, taking into account width of peak.

4. CONCLUSIONS

The size dependence of the Fermi energy of spherical metal nanoparticles is calculated. It has been shown that taking into account the model of the finite potential well leads to a decrease in the value of the Fermi energy level. Increasing the radius of the particle leads to a decrease in the period and amplitude of oscillations, the values of which approach the value of the Fermi energy in a 3D metal.

The conductivity tensor for spherical metal nanoparticles is introduced and its diagonal components are calculated within the model of the potential well of finite depth. The evolution of the frequency dependences of the real and imaginary parts of the optical conductivity under variation of the radius has been analyzed.

It has been shown that the imaginary parts of the optical conductivity are alternating functions of frequency, while the real parts are nonnegative in the entire investigated frequency range. It has been established that, with an increase in the radius of a nanoparticle, the maxima of the real and imaginary parts of the optical conductivity components shift to the region of lower frequencies and the maxima merge with each other, which is due to an increase in the number of size quantization levels, and, consequently, the number of possible transitions between them.

The components of the optical conductivity were calculated for Ag, Cu and Al particles. The differences in the character of the frequency dependences of nanoparticles of various metals are caused by the differences in the relaxation times of conduction electrons.

REFERENCES

1. N.L. Dmitruk, S.Z. Malinich, *Ukr. J. Phys.* **9** No 1, 3 (2014).
2. V.I. Balykin, P.N. Melentiev, *Phys. Usp.* **61**, 133 (2018).
3. V.V. Kulish, *J. Nano- Electron. Phys.* **3** No 3, 105 (2011).
4. V.M. Shalaev, *Nat. Photon.* **1**, 41 (2007).
5. J.N. Anker, W.P. Hall, O. Lyandres, N.C. Shah, J. Zhao, R.P. Van Duyne, *Nat. Mater.* **7**, 442 (2008).
6. N.I. Zheludev, *J. Opt. A: Pure Appl. Opt.* **8**, S1 (2006).
7. K.F. MacDonald, Z.L. Sámson, M.I. Stockman, N.I. Zheludev, *Nat. Photon.* **3**, 55 (2009).
8. R.B. Nielsen, M.D. Thoreson, W. Chen, A. Kristensen, J.M. Hvam, V.M. Shalaev, A. Boltasseva, *Appl. Phys. B* **100**, 93 (2010).
9. X. Huang, P.K. Jain, I.H. El-Sayed, *Nanomedicine* **2**, 681 (2007).
10. O.L. Muskens, N. Del Fatti, F. Vallee, J.R. Huntzinger, P. Billaud, M. Broyer, *Appl. Phys. Lett.* **88**, 063109 (2006).
11. P. Stoller, V. Jacobsen, V. Sandoghdar, *Opt. Lett.* **31** No 16, 2474 (2006).
12. R.G. Freeman, K.C. Grabar, K.J. Allison, R.M. Bright, J.A. Davis, A.P. Guthrie, M.B. Hommer, M.A. Jackson, P.C. Smith, D.G. Walter, M.J. Natan, *Science* **267**, 1629 (1995).

13. R.P. Andres, J.D. Bielefeld, J.I. Henderson, D.B. Janes, V.R. Kolagunta, C.P. Kubiak, W.J. Mahoney, R.G. Osifchin, *Science* **273**, 1690 (1996).
14. P.M. Tomchuk, N.I. Grigorchuk, *Phys. Rev. B* **73**, 155423 (2006).
15. A.L. González, J.A. Reyes-Esqueda, Cecilia Noguez, *J. Phys. Chem. C* **112** No 19, 7356 (2008).
16. P.M. Tomchuk, D.V. Butenko, *Ukr. J. Phys.* **60** No 10, 1043 (2015).
17. N.I. Grigorchuk, *J. Phys. Stud.* **20** No 1/2, 1701 (2016) [In Ukrainian].
18. N.I. Grigorchuk, *Metallofiz. Nov. Tekhnol.* **38** No 6, 717 (2016).
19. R. Ruppin, *Phys. Rev. B* **45**, 11209 (1992).
20. W.C. Huang, J.T. Lue, *Phys. Rev. B* **49**, 17279 (1994).
21. G.N. Blackman, D.A. Genov, *Phys. Rev. B.* **97**, 115440 (2018).
22. R. Ruppin, H. Yatom, *Phys. status solidi B* **74**, 647 (1976).
23. D.M. Wood, N.W. Ashcroft, *Phys. Rev. B* **25**, 6255 (1982).
24. V.P. Kurbatsky, V.V. Pogosov, *Phys. Rev. B* **81**, 155404 (2010).
25. A.A. Koval, A.V. Korotun, *Phys. Met. Metallogr.* **122** No 3, 230 (2021).
26. N.W. Aschcroft, N.D. Mermin, *Solid State Physics, Vol. 1* (Holt, Renehart, and Winston: New York: 1976).

Оптична провідність сферичної металевої наночастинки з урахуванням розмірної залежності енергії Фермі

А.О. Коваль[1,2]

[1] *Національний університет "Запорізька політехніка", вул. Жуковського, 64, 60063 Запоріжжя, Україна*
[2] *Науково-виробничий комплекс "Іскра", вул. Магістральна, 84, 69071 Запоріжжя, Україна*

У роботі досліджено взаємодію електромагнітних хвиль зі сферичною металевою наночастинкою. В рамках моделі сферично-симетричної потенційної ями кінцевої глибини розраховано розмірну залежність енергії Фермі електронів провідності. Показано, що врахування моделі сферичної потенційної ями кінцевої глибини призводить до зменшення значення енергії Фермі при зберіганні загального характеру розмірних залежностей. У наближенні діагонального відгуку отримано вирази та розраховано діагональні компоненти тензора оптичної провідності сферичної металевої наночастинки радіусом r_0. Досліджено вплив варіації величини ефективного радіусу і матеріалу сферичної наночастинки на частотні залежності дійсної та уявної частин оптичної провідності. Шляхом порівняння результатів розрахунків діагональної компоненти тензора оптичної провідності сферичної наночастинки та циліндричного нанодроту для Cu встановлено вплив розмірності систем. Результати розрахунків демонструють сильну розмірну і частотну залежність дійсної та уявної частин оптичної провідності. Обчислення проведені для сферичних наночастинок Ag, Cu і Al. Відмінності в результатах для сферичних наночастинок Ag, Cu і Al пояснюються різними значеннями часу релаксації електронів провідності.

Ключові слова: Енергія Фермі, Металева наночастинка, Оптична провідність, Розмірне квантування.